POLITECNICO DI TORINO
Repository ISTITUZIONALE

Gold Nanostars based Microfluidic Optical Fiber Sensor for Enhanced Ethanol Detection

Original
Gold Nanostars based Microfluidic Optical Fiber Sensor for Enhanced Ethanol Detection / Russo, S., Boetti, N.G., Giardino, M., Chiavaioli, F., Janner, D.. - In: IEEE SENSORS JOURNAL. - ISSN 1530-437X. - (2026), pp. 1-8. [10.1109/JSEN.2026.3724806]

Availability:
This version is available at: 11583/3016181 since: 2026-09-30T21:04:51Z

Publisher:
Institute of Electrical and Electronics Engineers - IEEE

Published
DOI:10.1109/JSEN.2026.3724806

Terms of use:

This article is made available under terms and conditions as specified in the corresponding bibliographic description in the repository

Publisher copyright

(Article begins on next page)

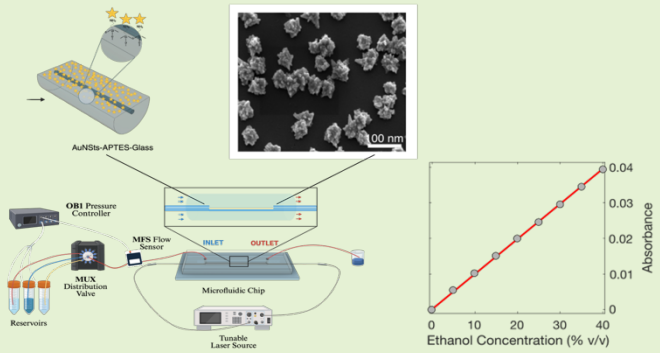
26 November 2026

This article has been accepted for publication in IEEE Sensors Journal. This is the author's version which has not been fully edited and content may change prior to final publication. Citation information: DOI 10.1109/JSEN.2026.3724806

Gold Nanostars based Microfluidic Optical Fiber Sensor for Enhanced Ethanol Detection

Sharon Russo, Nadia G Boetti, Matteo Giardino, Francesco Chiavaioli, Davide Janner

***Abstract*— In this work, we present an ethanol sensor based on a D-shaped optical fiber functionalized with a nanostructured layer of gold nanostars (AuNSs). The functionalization was achieved via a seed-mediated growth method, enabling uniform and controlled nanoparticle deposition on the fiber surface. The sensor was integrated into a custom-designed microfluidic chip, allowing precise control of analyte delivery and ensuring highly reproducible measurements. The sensing mechanism relies on the interaction between the evanescent field of the D-shaped fiber and the AuNSs, which enhances light–matter interaction and increases sensitivity to refractive index variations induced by ethanol concentration changes. The device exhibited a highly linear response (R^2 = 99.960) over a concentration range of 0–40%, with a detection limit of 0.07% and a response time of approximately 10 s. The combination of nanostructured plasmonic materials and microfluidic integration results in improved sensitivity, repeatability, and response speed. These results demonstrate the potential of D-shaped fiber platforms functionalized with gold nanostructures for the development of compact and efficient chemical sensing systems.**



***Index Terms*— D-shaped fiber, Gold Nanostars, Ethanol, Sensing, Microfluidic system**

I. Introduction

Ethanol (ethyl alcohol) is a colorless, volatile, and flammable compound widely used for its solvent properties and role as a renewable resource. It is a key component in industries such as pharmaceuticals, cosmetics, disinfectants, and biofuels [1], [2], [3]. Because of its broad use, accurate ethanol detection is important for environmental monitoring, food and beverage quality control [4], biofuel optimization, medical diagnostics [5], and pharmaceutical manufacturing. In biofuel production, monitoring ethanol helps optimize fermentation and ensure safety by reducing fire and explosion risks [2]. In healthcare, it supports the detection of alcohol intoxication and chronic use through biomarkers like ethyl glucuronide (EtG) and ethyl sulfate (EtS) [6]. In pharmaceuticals, precise measurement is essential since ethanol is commonly used as a solvent and must meet regulatory standards [7]. Several analytical techniques have been developed for ethanol detection. The most common methods rely on gas chromatography, UV/NIR spectroscopy, enzymatic measurement, and refractive index (RI) analysis. These methods, while effective, suffer from limitations such as low sensitivity and reproducibility, complex instrumentation requirements, high costs, and a lack of real-time monitoring capabilities [3]. Gas chromatography, for example, requires extensive sample preparation and sophisticated laboratory equipment, making it unsuitable for continuous or portable sensing applications [8]. Similarly, spectroscopic and enzymatic techniques often require expensive reagents and extensive calibration procedures, limiting their practicality for widespread use [9], [10]. To overcome these challenges, fiber optic sensors have gained significant attention due to their many advantages, such as unique light control, low weight and compact size, immunity to electromagnetic interference, high RI sensitivity, their potential of being real time, remote sensing and capability for multi-analyte detection [3], [11], [12], [13].

Optical fiber sensors have been widely exploited for ethanol sensing using absorption, interferometric, fiber grating, and plasmonic techniques. Many reported designs enhance evanescent field interaction through structures such as tapered fibers, U-bent fibers, and photonic crystal fibers, often combined with nanomaterials like graphene, graphene oxide, CNTs, MoS_2, gold nanoparticles, and hydrogels. Tapered or bent geometries improve sensitivity by increasing evanescent field exposure, but they often suffer from reduced mechanical strength and poor environmental stability. For example,

XXXX-XXXX © XXXX IEEE. Personal use is permitted, but republication/redistribution requires IEEE permission.
See http://www.ieee.org/publications_standards/publications/rights/index.html for more information.
This work is licensed under a Creative Commons Attribution-NonCommercial-NoDerivatives 4.0 License.
For more information, see https://creativecommons.org/licenses/by-nc-nd/4.0/

This article has been accepted for publication in IEEE Sensors Journal. This is the author's version which has not been fully edited and
content may change prior to final publication. Citation information: DOI 10.1109/JSEN.2026.3724806

meander-shaped fibers can achieve sub-0.2% detection over 0–10% ethanol but require complex fabrication and lack robustness [14]. Similarly, tapered multimode fibers show sensitivities of 0.22–0.34 ΔA%/ΔC depending on coatings, though fragility remains a key limitation [15], [16], [17].

A comprehensive comparison between the proposed ethanol sensor and previously reported absorption-based optical fiber sensors is summarized in Table 1. Compared to other types of optical fiber, D-shaped fibers have emerged as particularly effective in sensing due to their flat polished surface, which enhances light–environment interaction and allows easy surface functionalization. This geometry improves sensitivity by enabling a larger portion of the optical field to interact with the functional coating and surrounding medium [13],[14], [19],[20],[21]. In previous work, CNT-coated D-shaped fibers achieved a sensitivity of 0.0409 dB/% for ethanol sensing, benefiting from dipole interactions between COOH groups and ethanol molecules [22]. Another widely used approach is metal deposition on the D-shaped surface (e.g., gold or silver) to excite surface plasmon resonance (SPR) [23]. Recent D-shaped SPR fiber sensors employing optimized plasmonic coatings and dielectric overlayers have demonstrated enhanced refractive index sensitivity and sharper resonance characteristics, while multilayer gold/graphene/polymer structures achieved sensitivities of about 0.25 nm/% over a 0–90% ethanol concentration range [24], [25], [26], [27].

To produce high-quality films with controlled thickness and composition, different deposition techniques are available. Among these, sputtering is the most employed, effective and reliable. However, this method suffers from many limitations such as complex instrumentation, spitting defects, and poor adhesion of the film to the substrate. Metallic nanostructures are an alternative to thin films due to their strong Localized Surface Plasmon Resonance (LSPR). LSPR is highly sensitive to changes in the surrounding refractive index, enabling applications in biomolecule detection and environmental sensing [28], [29], [30]. Gold nanoparticles have size- and shape-dependent optical properties, with gold nanostars (AuNSs) exhibiting higher refractive index sensitivity than conventional spherical gold nanoparticles (AuNPs) owing to their sharp tips and the strong *lightning rod effect*. Their branched morphology also provides a larger active surface for functionalization and enhances the interaction between the plasmonic field and the surrounding medium. Their plasmonic absorption can be tuned from the visible to the near-infrared range, while their chemical stability and biocompatibility make them well suited for optical ethanol sensing [31]. Optical fiber sensors provide fast, compact, real-time sensing but often face challenges with reproducibility and sample delivery. Integrating them with microfluidic platforms, miniaturized systems that precisely handle tiny fluid volumes, improves control, reduces reagent consumption, speeds up analysis, and enables highly sensitive measurements. This combination, known as optofluidics, enhances sensing performance across biological, environmental, and food-monitoring applications [32]. Embedding an optical fiber within a microfluidic channel enables monitoring of optical signals in a confined, controlled environment, where analyte–sensor interactions occur at the microscale. Moreover, the microfluidic platform provides direct access to the fiber surface, facilitating surface modification and functionalization for enhanced biosensing [33]. The current literature reports on a limited number of optical ethanol sensors that simultaneously ensure rapid and straightforward fabrication, reproducible and reliable performance, and functionalization with safe and biocompatible sensing materials. This gap highlights the need to develop sensors capable of meeting all these requirements.

The proposed sensor combines a D-shaped fiber platform with a nanostructured layer of gold nanostars (AuNSs), integrated within a microfluidic system. The D-shaped geometry provides a stable and reproducible evanescent field interaction without the mechanical fragility associated with tapered or heavily bent fibers. The Au nanostars significantly enhance local electromagnetic fields, improving sensitivity to refractive index variations induced by ethanol concentration changes. Furthermore, the integration with a microfluidic platform ensures precise control of analyte delivery, reduces contamination effects, and enables highly repeatable measurements.

TABLE 1 : LITERATURE COMPARISON BETWEEN THIS WORK AND PREVIOUS ETHANOL OPTICAL FIBER SENSORS

Geometry	Coating	Range	Sensitivity	Response Time	Ref
Tapered (Silica MM)	Graphene, Graphene Oxide (GO)	5-40%	0.829/vol% for graphene and 1.330/vol % for GO-coated	15 s for GO and 25 s for graphene coated sensor	[16]
U-bent (MM PCS fiber)	Gold nanoparticles on Tungsten disulphide	10-80%	0.65 (ΔA%/ΔC%)	/	[34]
Tapered (MM fiber)	Hydrogel	0–62.2 %	LOD 0.4 vol%	2 min	[15]
Tapered U-bent (Silica MM fiber)	MoS2	0-100%	0.34 (ΔA%/ΔC%)	0.5 s	[35]

XXXX-XXXX © XXXX IEEE. Personal use is permitted, but republication/redistribution requires IEEE permission.
See http://www.ieee.org/publications_standards/publications/rights/index.html for more information.
This work is licensed under a Creative Commons Attribution-NonCommercial-NoDerivatives 4.0 License.
For more information, see https://creativecommons.org/licenses/by-nc-nd/4.0/

This article has been accepted for publication in IEEE Sensors Journal. This is the author's version which has not been fully edited and content may change prior to final publication. Citation information: DOI 10.1109/JSEN.2026.3724806

D-shaped (Silica SMF-28)	AuNSs	0-40%	0.11 (ΔA%/ΔC%) LOD 0.07%	10 s	This work

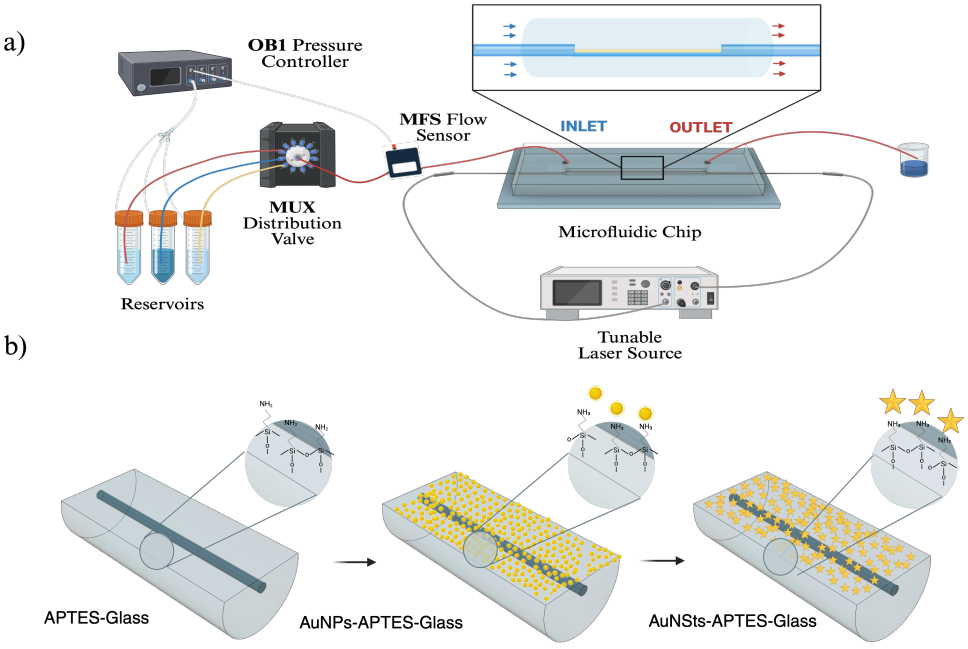
II. Materials and Methods

A. Experimental setup

The experimental setup for the proposed ethanol sensor is shown in Fig. 1a. A commercially available D-shaped SMF-28 single-mode optical fiber (Phoenix Photonics Ltd., UK), operating at 1550 nm, was used. The polished region was 10 mm long with a depth of approximately 65 µm. The fiber was integrated into a custom-designed microfluidic chip through a dedicated microchannel, enabling controlled interaction between the guided optical mode and the liquid analyte.

Sensor characterization was performed using an Elveflow pressure-driven microfluidic system comprising an OB1 Pressure Controller, a MUX Distribution Valve, and an MFS Flow Sensor. The OB1 Pressure Controller regulated the flow by applying controlled air pressure to sealed reservoirs. The MUX Distribution Valve enabled automated selection of the desired solution without altering the fluidic connections, ensuring rapid switching between solutions. The MFS Flow Sensor continuously monitored the flow rate and provided real-time feedback to the OB1 through a closed-loop control algorithm, maintaining a constant flow rate throughout the measurements. The microfluidic chip was fabricated by first designing and 3D-printing a negative mold using a Formlabs Form 3+ printer and Clear V4 resin. PDMS (Sylgard 184) was prepared in a 10:1 base-to-curing-agent ratio, degassed, cast into the mold, and cured at 80°C for 2 h. The cured PDMS structure was then plasma-treated and bonded to a glass microscope slide to create a sealed microfluidic device.

The microfluidic channel was approximately 50 mm long with a cross-section of 1 mm × 1 mm, leveraging an effective sensing volume of approximately 10 µL. Before testing, the D-shaped fiber was functionalized and inserted into the chip channel to ensure precise alignment and mechanical stability. The ethanol sensing experiments involved flowing ethanol solutions with concentrations ranging from 0% to 40% through the chip. Each concentration was introduced for a duration of 180 seconds at a constant flow rate of 500 µL/min. The temperature was kept constant at 22 °C using a Peltier cell located beneath the base of the microfluidic chip and controlled by a TEC controller (TEC-1091-PT100-SCREW, Meerstetter.ch). Temperature feedback was provided by a Pt100 sensor embedded in the PDMS layer, close to the channel, ensuring precise thermal regulation via closed-loop control of the Peltier element. Nitrogen gas was initially flowed through the microchannel, followed by a flow of ultrapure water to acquire reference signal (baseline). Three independently fabricated AuNS-coated D-shaped optical fiber sensors were characterized to evaluate the reproducibility of the proposed sensing platform. The repeatability was assessed by performing three independent repeated measurements at representative ethanol concentrations (10%, 20%, and 40% v/v). Optical measurements were performed using an Agilent 8163A Lightwave Multimeter. The laser source, set to 1550 nm, was fiber-coupled to an FC/PC terminated single-mode fiber. This input fiber was fusion-spliced to one end of the D-shaped fiber sensor. The output end of the sensor was similarly fusion spliced to another FC/PC SM fiber, which was connected to a power meter via an Agilent 81000FA FC Connector Adapter.



This work is licensed under a Creative Commons Attribution-NonCommercial-NoDerivatives 4.0 License.
For more information, see https://creativecommons.org/licenses/by-nc-nd/4.0/

This article has been accepted for publication in IEEE Sensors Journal. This is the author's version which has not been fully edited and
content may change prior to final publication. Citation information: DOI 10.1109/JSEN.2026.3724806

Fig. 1. (a) The experimental setup for the proposed ethanol sensor; (b) The D-shaped fiber section functionalization process for enhanced ethanol detection

B. D-shaped fiber functionalization process

A nanostructured gold layer was deposited on the D-shaped fiber to increase absorption of the evanescent wave field in the surrounding medium and thereby enhance sensitivity to ethanol concentration variations. The layer was obtained through the seed-mediated growth method. Initially, spherical gold nanoparticle seeds with a nominal diameter of 10 nm were used. These seeds were grown using a solution containing polyvinylpyrrolidone (PVP), dimethylformamide (DMF), and a gold precursor, resulting in a solution of AuNSs.

All the chemicals, including Gold Nanoparticles (AuNPs; diameter of 10 nm, stabilized in citrate buffer), (3-Aminopropyltriethoxysilane (APTES), Polyvinylpyrrolidone (PVP, average MW = 10 000), N,N-Dimethylformamide (DMF) and Gold (III) chloride solution were purchased from Sigma Aldrich (Merck, Darmstadt, Germany).

The D-shaped fiber, before insertion in the microfluidic chip, was cleaned with ethanol (EtOH) and hydrolyzed with a base piranha solution, a mixture of ammonium hydroxide (NH_4OH) and hydrogen peroxide (H_2O_2, 30 % (w/w) in H_2O) with a volume ratio of 3:1. The solution was heated at 60°C and the fiber was soaked in the solution for 20 minutes. After immersion in piranha solution, the D-shaped fiber was inserted in a Teflon tube for seed deposition. First, it was silanized by treating it with a 3% (v/v) APTES solution in ethanol (EtOH) for 90 minutes, thereby forming surface monolayers bearing amino groups. The fiber was later washed with Ethanol and dried under nitrogen. Subsequently, 1 mL of gold seeds was introduced into the tube for deposition onto the fiber surface for approximately 4 hours. The fiber was again washed with EtOH to remove any unbound seeds and then dried under N_2.

The AuNSs growth solution was prepared by carefully mixing 55 µL of a solution of 100 mM $HAuCl_4$ with 20 mL of PVP 10 mM in DMF. [31], [36] The solution was kept under stirring at room temperature for about 5 minutes. The solution was subsequently introduced into the Teflon tube, where the fiber was held, allowing gold seeds to grow into stars. The color of the solution changed from transparent to black in about 30 minutes. Finally, the fiber was washed again with EtOH and dried with N_2. The fiber was removed from the tube and inserted in the microfluidic chip for the following testing procedures performed with the microfluidic platform. This process is sketched in Fig. 1b.

III. Results and Discussion

The nanostructured layer of gold nanostars was characterized using SEM analysis to observe both the distribution density on the D-shaped fiber and the morphology of the nanoparticles. The reported average particle diameter, and surface coverage were obtained by averaging measurements from multiple SEM images of D-shaped regions on the three independently fabricated AuNS-coated fiber samples. Through precise control over the deposition parameters, specifically the deposition time and the concentration of chemical reagents, it was possible to achieve an optimal surface coverage and spatial distribution of AuNSs on the surface of the D-shaped optical fiber. Achieving a uniform and high-density distribution of AuNSs is critical for enhancing the sensitivity and repeatability of the sensor. To determine the most suitable seed size for AuNSs growth, two different AuNP seed diameters were investigated: 10 nm and 20 nm. Experimental results demonstrated that the 10 nm diameter seeds (Fig. 1S b) yielded a more uniform and denser distribution of Au seeds on the fiber surface, compared to the 20 nm seeds (Fig. 1S a), which showed relatively sparser and less homogeneous surface coverage. This difference can stem from the adsorption kinetics of AuNPs on the glass surface. At this stage, repulsive electrostatic interactions dominate and are highly dependent on nanoparticle size. The larger seed size likely increases the interparticle distance due to these repulsive forces, resulting in less effective surface coverage [37]. In addition to seed optimization, the molar concentrations of the gold precursor ($HAuCl_4$) and the reduction agent, the PVP polymer dissolved in DMF, were carefully adjusted. Special attention was paid to keep an appropriate [Au]/[PVP] ratio, which is essential for the controlled reduction of gold ions and the anisotropic growth of star-shaped branches on the seed nanoparticles [38].

The mean size of the stars obtained after 30 minutes of growth was about 50 nm in diameter (Fig. 2a and 2b). SEM image analysis estimated a surface coverage of approximately 35% for the gold structures on the fiber surface. The coverage was quantified by calculating the area fraction from binary masks generated from the SEM images. A microscope glass slide was cut into a 1 × 1 cm square and subjected to the same deposition and growth procedures for subsequent UV-Vis-NIR and FTIR spectroscopic analysis. The corresponding UV-Vis-NIR spectrum is shown in Fig. 2c. The graph clearly underscores the resonance peaks corresponding to the different plasmonic modes excited within this nanostructure. Gold nanospheres typically exhibit a plasmonic resonance peak at approximately 550 nm, corresponding to the collective oscillation of conduction electrons in the nanoparticle core. In this case, the peak shifts to the red and becomes significantly weaker, primarily due to the larger core diameter and the dominance of the longitudinal plasmon mode of the AuNSs.

A pronounced peak appears around 700 nm, which is attributed to the longitudinal plasmon resonance arising from the branches of the nanostars. This resonance corresponds to a dipolar mode, driven by the oscillation of the free electron cloud along the length of the spikes. The sharp tips of the nanostars act as individual plasmonic hotspots, resulting in strong local electromagnetic field enhancements [36], [39]. Although the main plasmonic resonance of the synthesized AuNSs is centered around 700 nm, the UV–Vis–NIR and FTIR spectra reveal a broad extinction profile extending into the near-infrared region, with measurable absorption at 1550 nm (Fig. 2d). Therefore, the plasmonic coating remains optically active at the interrogation wavelength, where the optical fiber operates in the single-mode regime. Preliminary experiments with a bare D-shaped optical fiber showed no detectable response to ethanol concentration under the adopted interrogation conditions, whereas AuNS functionalization enabled a clear and reproducible sensing signal.

This work is licensed under a Creative Commons Attribution-NonCommercial-NoDerivatives 4.0 License.
For more information, see https://creativecommons.org/licenses/by-nc-nd/4.0/

This article has been accepted for publication in IEEE Sensors Journal. This is the author's version which has not been fully edited and content may change prior to final publication. Citation information: DOI 10.1109/JSEN.2026.3724806

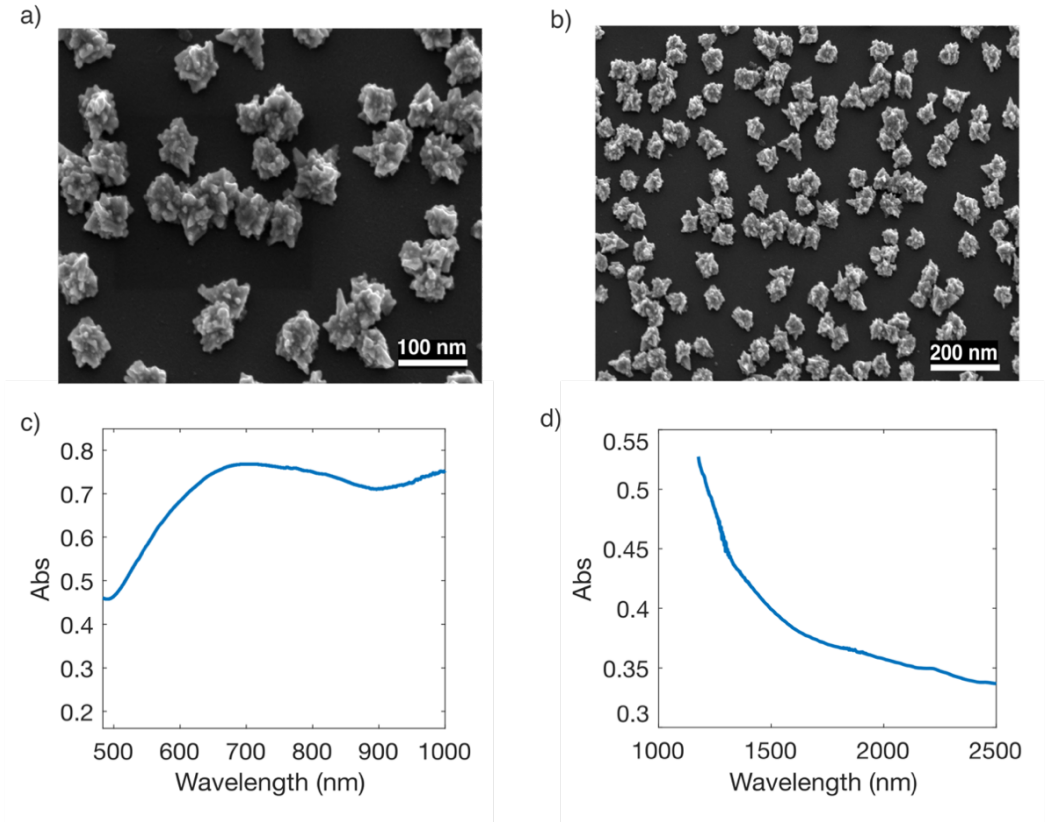


Fig. 2. (a) 50K, (b) 25K magnification SEM images of AuNSs deposited on the D-shaped fiber after 30 minutes of growth with different magnification. (c) UV-Vis-NIR (d) FTIR spectra of AuNSs grown on a flat glass

The performance of the AuNSs coated D-shaped fiber optical sensor was assessed by analyzing its absorbance and transmitted power characteristics under varying ethanol concentrations. The microfluidic platform allowed for the sequential switching between the different ethanol concentration solutions, guaranteeing a controlled, fast, and automated testing of the transmitted power changes in the D-shaped fiber due to the increasing RI of the dielectric surrounding medium. Fig. 3a accounts for the real-time sensorgram, showing the fiber-transmitted power as a function of time during the flow of different ethanol solutions over the sensing region. A stepwise decrease in transmitted power is observed with increasing ethanol concentration. This repeatable behavior indicates the expected optical attenuation resulting from ethanol's interaction with the evanescent field of the D-shaped fiber sensor. In Fig. 3b, the calibration curve of the sensor is reported. The graph illustrates the relationship between ethanol concentration and light absorbance. The reported values correspond to the average response of the three sensors, and the error bars represent the standard deviation among the devices. A clear linear correlation is observed, with absorbance increasing proportionally to ethanol concentration in the range of 0% to 40%. This range was selected because the refractive index of ethanol–water mixtures is approximately linear within this interval, whereas higher ethanol concentrations are known to exhibit nonlinear refractive index behavior due to changes in the ethanol–water hydrogen-bonding network. [40] The fitted calibration curve demonstrates high linearity (R-squared = 99.96%), one of the highest reported in the literature, indicating strong accuracy and reliability of the sensor for ethanol detection. The estimated Limit of Detection (LOD) of the proposed ethanol sensor calculated as three times the standard deviation of the blank point (i.e., 0% ethanol concentration) [41] is 0.07 % of ethanol and it exhibited an absorbance sensitivity per % change in concentration of 0.11 %A/%C. Moreover, the use of a narrowband laser centered at 1550 nm enabled detection of optical power variations at a single wavelength, eliminating the need for spectral integration and ensuring reliable measurements. The observed changes in absorbance and transmitted power are attributed to variations in the RI of the surrounding environment. As the ethanol concentration increases, the RI of the surrounding medium shifts from 1.3180 to 1.3298 at 1550 nm for 0 to 40% (v/v) of ethanol. This increase affects the interaction between the evanescent field and the guided optical mode in the D-shaped fiber. The evanescent wave, which extends beyond the fiber core into the surrounding medium, undergoes a shift in penetration depth and intensity as the RI varies. When the ethanol concentration increases, the RI difference between the fiber core and the surrounding medium decreases, modifying the light confinement. The RI of the external medium affects the TIR phenomenon inside the fiber. In standard conditions, light propagates through the fiber due to TIR at the fiber-medium interface. However, as the surrounding RI increases, the critical angle for TIR is reduced, meaning that a larger portion of the light energy is lost into the external

This work is licensed under a Creative Commons Attribution-NonCommercial-NoDerivatives 4.0 License.
For more information, see https://creativecommons.org/licenses/by-nc-nd/4.0/

This article has been accepted for publication in IEEE Sensors Journal. This is the author's version which has not been fully edited and
content may change prior to final publication. Citation information: DOI 10.1109/JSEN.2026.3724806

medium through the evanescent field [20]. This effect leads to increased optical losses, as evidenced by a reduction in transmitted power in the experimental results. The AuNSs coating on the fiber D-shape section, where the cladding removal allowed the evanescent wave to reach the fiber's surface, empowers the light-matter interaction given a stronger interaction between the evanescent field and the external medium, extending the penetration depth of the evanescent field and improving the sensor's capability to detect small changes in ethanol concentration, as even minor RI variations lead to detectable power losses. The stepwise behavior in the transmitted power (Fig. 3a) suggests that the sensor reacts promptly to changes in ethanol concentration. The smooth transitions between power levels indicate a fast adaptation of the sensor to new ethanol concentrations with low measurement noise, as indicated by a mean standard deviation of 0.02 µW. The relative standard deviation (RSD) between repeated measurements was approximately 1.3% at 10% and 20% ethanol and 0.6% at 40% ethanol, while the short-term signal fluctuations within each acquisition remained below 0.4%, confirming the good repeatability and stability of the sensing platform.To evaluate the system response time, the power decay observed during the transition from flowing water to a 10% ethanol solution was fitted to an exponential decay model via nonlinear least-squares regression. The resulting time constant was 10.57 s, and the experimental data together with the corresponding fitted curve are presented in Fig. 2S. This value represents the overall response of the integrated microfluidic sensing platform, including both fluid transport and the intrinsic optical response of the sensor under the adopted flow conditions. The probe was rinsed with deionized water after each ethanol measurement to restore the baseline signal. The recovery dynamics were found to be strongly dependent on the flow rate, being slower for the condition shown in Fig. 3c (500 µL /min) and faster for that in Fig. 3d (1 mL/min). During a transitional phase of partially mixing between ethanol and water within the microfluidic channel, the signal progressively returned close to the baseline level in both cases; however, a slight drift of approximately 10% relative to the initial signal was observed after exposure to the 10% ethanol solution under the lower flow-rate condition (Fig. 3c). For the higher flow rate (Fig. 3d), the recovery time was estimated to be approximately 20 s, obtained by fitting the transient response with an exponential decay model. This rapid response is crucial for real-time applications, where short detection and recovery time are necessary. Additionally, the fast response time highlights the efficiency of the microfluidic platform in enabling rapid solution exchange without inducing instability in the measurement process. This RI-dependent response, combined with the microfluidic platform and the nanostructured gold coating, enhances the sensor's capability to detect ethanol concentrations with high sensitivity, making it suitable for real-time monitoring applications.

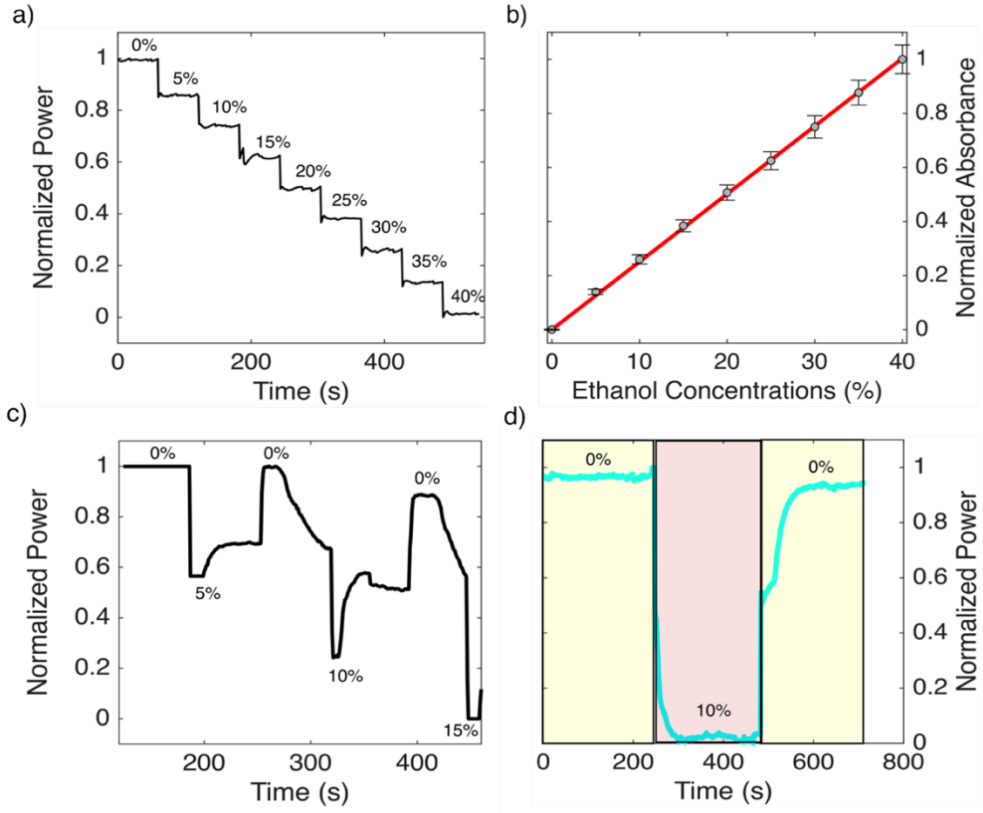


Fig. 3. (a) Sensorgram showing the D-shaped fiber transmitted power reduction for each ethanol concentration in time. (b) Calibration curve of the D-shaped fiber sensor for ethanol concentration ranging from 0% to 40 %. Recovery of the sensor after exposure to ethanol solution at a flow rate of c) 500 µL/min and of d) 1 mL/min.

This work is licensed under a Creative Commons Attribution-NonCommercial-NoDerivatives 4.0 License.
For more information, see https://creativecommons.org/licenses/by-nc-nd/4.0/

This article has been accepted for publication in IEEE Sensors Journal. This is the author's version which has not been fully edited and
content may change prior to final publication. Citation information: DOI 10.1109/JSEN.2026.3724806

IV. Conclusion

A D-shaped optical fiber sensor functionalized with a nanostructured layer of gold nanostars (AuNSs) was successfully developed for ethanol concentration monitoring. By combining the enhanced evanescent-field interaction of the D-shaped fiber with the strong plasmonic response of AuNSs, the proposed platform achieved high refractive index sensitivity, improving the detection of ethanol-induced refractive index variations. Integrated with a pressure-driven microfluidic system, the sensor exhibited a highly linear response over the 0–40% (v/v) ethanol concentration range (R^2 = 99.960), a detection limit of 0.07%, and a response time of approximately 10 s, while maintaining excellent stability and repeatability. The microfluidic platform ensured precise flow-rate control, automated switching between ethanol solutions, and reproducible analyte delivery, contributing to the robustness of the measurements. Overall, the proposed sensing platform combines high sensitivity, rapid response, and low-cost fabrication, making it a promising solution for real-time ethanol monitoring in biomedical, environmental, and industrial applications. Future work will focus on integrating selective functional coatings to improve analyte specificity and extend the sensing capabilities of the platform.

References

[1] University of Zagreb, Faculty of Food Technology and Biotechnology, Pierottijeva 6, 10000 Zagreb, Croatia *et al.*, «Bioethanol Production from Renewable Raw Materials and its Separation and Purification: a Review», *Food Technol. Biotechnol.*, vol. 56, fasc. 3, 2018, doi: 10.17113/ftb.56.03.18.5546.

[2] «The Editors of Encyclopaedia Britannica. Encyclopedia Britannica. https://www.britannica.com/science/ethanol».

[3] S. F. Memon, R. Wang, B. Strunz, B. S. Chowdhry, J. T. Pembroke, e E. Lewis, «A Review of Optical Fibre Ethanol Sensors: Current State and Future Prospects», *Sensors*, vol. 22, fasc. 3, p. 950, gen. 2022, doi: 10.3390/s22030950.

[4] A. R. Mansur, J. Oh, H. S. Lee, e S. Y. Oh, «Determination of ethanol in foods and beverages by magnetic stirring-assisted aqueous extraction coupled with GC-FID: A validated method for halal verification», *Food Chemistry*, vol. 366, p. 130526, gen. 2022, doi: 10.1016/j.foodchem.2021.130526.

[5] B. Le Daré e T. Gicquel, «Therapeutic Applications of Ethanol: A Review», *J Pharm Pharm Sci*, vol. 22, pp. 525–535, ott. 2019, doi: 10.18433/jpps30572.

[6] K. D. Tawiah, S. B. Riley, e M. M. Budelier, «Biomarkers and Clinical Laboratory Detection of Acute and Chronic Ethanol Use», *Clinical Chemistry*, vol. 68, fasc. 5, pp. 635–645, mag. 2022, doi: 10.1093/clinchem/hvac004.

[7] W. A. Parker, «Alcohol-Containing Pharmaceuticals», *The American Journal of Drug and Alcohol Abuse*, vol. 9, fasc. 2, pp. 195–209, gen. 1982, doi: 10.3109/00952998209002622.

[8] M.-L. Wang, Y.-M. Choong, N.-W. Su, e M.-S. Lee, «A rapid method for determination of ethanol in alcoholic beverages using capillary gas chromatography», *Journal of Food and Drug Analysis*, vol. 11, fasc. 2, lug. 2020, doi: 10.38212/2224-6614.2710.

[9] C. L. Sanford, B. A. Mantooth, e B. T. Jones, «Determination of Ethanol in Alcohol Samples Using a Modular Raman Spectrometer», *J. Chem. Educ.*, vol. 78, fasc. 9, p. 1221, set. 2001, doi: 10.1021/ed078p1221.

[10] S. Castritius, A. Kron, T. Schäfer, M. Rädle, e D. Harms, «Determination of Alcohol and Extract Concentration in Beer Samples Using a Combined Method of Near-Infrared (NIR) Spectroscopy and Refractometry», *J. Agric. Food Chem.*, vol. 58, fasc. 24, pp. 12634–12641, dic. 2010, doi: 10.1021/jf1030604.

[11] C. McDonagh, C. S. Burke, e B. D. MacCraith, «Optical Chemical Sensors», *Chem. Rev.*, vol. 108, fasc. 2, pp. 400–422, feb. 2008, doi: 10.1021/cr068102g.

[12] C. Chen *et al.*, «Evanescent wave-based optical biosensors for innovations, medical application and future perspectives», *Journal of Advanced Research*, p. S2090123225005053, lug. 2025, doi: 10.1016/j.jare.2025.07.007.

[13] D. Santano, A. B. Socorro, A. Giannetti, I. D. Villar, e F. Chiavaioli, «Simultaneous detection of inflammatory process indicators via *operando* dual lossy mode resonance-based biosensor», *OES*, vol. 4, fasc. 10, p. 250005, 2025, doi: 10.29026/oes.2025.250005.

[14] M. Fabian, E. Lewis, T. Newe, S. Lochmann, e I. Mueller, «Investigation of ethanol and methanol water mixtures in the visible wavelength area using fibre-optic evanescent field absorption sensors based on a u-shaped, a coil-shaped and a meander-shaped probe», in *2008 IEEE Sensors Applications Symposium*, Atlanta, GA: IEEE, feb. 2008, pp. 79–84. doi: 10.1109/SAS13374.2008.4472948.

[15] S. Hong *et al.*, «A hydrogel optical fibre sensor for rapid on-site ethanol determination», *Anal. Methods*, vol. 16, fasc. 5, pp. 780–785, 2024, doi: 10.1039/D3AY02092D.

[16] S. H. Girei, A. A. Shabaneh, H. Ngee-Lim, M. N. Hamidon, M. A. Mahdi, e M. H. Yaacob, «Tapered optical fiber coated with graphene based nanomaterials for measurement of ethanol concentrations in water», *Opt Rev*, vol. 22, fasc. 3, pp. 385–392, giu. 2015, doi: 10.1007/s10043-015-0075-8.

[17] Z. Li *et al.*, «Evanescent wave absorption sensor with direct-growth MoS_2 film based on U-bent tapered multimode fiber», *J. Phys. D: Appl. Phys.*, vol. 50, fasc. 31, p. 315302, ago. 2017, doi: 10.1088/1361-6463/aa7b06.

[18] F. De-Jun, Z. Mao-Sen, G. Liu, L. Xi-Lu, e J. Dong-Fang, «D-Shaped Plastic Optical Fiber Sensor for Testing Refractive Index», *IEEE Sensors J.*, vol. 14, fasc. 5, pp. 1673–1676, mag. 2014, doi: 10.1109/JSEN.2014.2301911.

[19] F. Chiavaioli e D. Janner, «Fiber Optic Sensing With Lossy Mode Resonances: Applications and Perspectives», *J. Lightwave Technol.*, vol. 39, fasc. 12, pp. 3855–3870, giu. 2021, doi: 10.1109/JLT.2021.3052137.

[20] A. K. Sharma, J. Gupta, e I. Sharma, «Fiber optic evanescent wave absorption-based sensors: A detailed review of advancements in the last decade (2007–18)», *Optik*, vol. 183, pp. 1008–1025, apr. 2019, doi: 10.1016/j.ijleo.2019.02.104.

[21] S. Dabagh, R. Singh, C. Borri, e F. Chiavaioli, «Functional Nanomaterial Coatings on Optical Fibers: Toward Enhanced Biosensing Performance», *IEEE Sens. Rev.*, vol. 2, pp. 157–169, 2025, doi: 10.1109/SR.2025.3568382.

[22] H. A. Zain, M. Batumalay, H. R. A. Rahim, M. Yasin, e S. W. Harun, «Single-walled carbon nanotubes coated D-shaped fiber for aqueous ethanol detection», *Optoelectron. Lett.*, vol. 18, fasc. 7, pp. 430–433, lug. 2022, doi: 10.1007/s11801-022-1166-y.

[23] S. Kumar, J. B. Maurya, B. Roumi, R. Abdi-Ghaleh, e Y. K. Prajapati, «D-shaped fiber optic plasmonic sensors using planar and grating structures of silver and gold: design and analysis», *Appl. Opt.*, vol. 62, fasc. 16, p. E130, giu. 2023, doi: 10.1364/AO.481145.

[24] V. Sharma, A. Kumar, S. Saharan, e S. Semwal, «Graphene/Au/MIP-Coated D-Shaped Optical Fiber–Based SPR Sensor for Ethanol Detection», *Plasmonics*, vol. 18, fasc. 5, pp. 1639–1649, ott. 2023, doi: 10.1007/s11468-023-01920-y.

[25] Y. Li *et al.*, «All-fiber-optic vector magnetic field sensor based on side-polished fiber and magnetic fluid», *Opt. Express*, vol. 27, fasc. 24, p. 35182, nov. 2019, doi: 10.1364/OE.27.035182.

[26] S. Han *et al.*, «In-line temperature-compensated vector magnetic field sensor with side-polished fiber», *Opt. Lett.*, vol. 48, fasc. 17, p. 4504, set. 2023, doi: 10.1364/OL.499780.

[27] P. Zhou *et al.*, «Orthogonal Double-Side-Polished Fiber SPR Sensor for Simultaneous Measurement of Refractive Index and Temperature», *IEEE Sensors J.*, vol. 26, fasc. 3, pp. 3872–3876, feb. 2026, doi: 10.1109/JSEN.2025.3641398.

[28] M. R. Kumalasari, R. Alfanaar, e A. S. Andreani, «Gold nanoparticles (AuNPs): A versatile material for biosensor application», *Talanta Open*, vol. 9, p. 100327, ago. 2024, doi: 10.1016/j.talo.2024.100327.

[29] M. Lu, C. Wang, R. Fan, M. Lin, J. Guang, e W. Peng, «Review of Fiber-Optic Localized Surface Plasmon Resonance Sensors: Geometries, Fabrication Technologies, and Bio-Applications»,

This work is licensed under a Creative Commons Attribution-NonCommercial-NoDerivatives 4.0 License.
For more information, see https://creativecommons.org/licenses/by-nc-nd/4.0/

This article has been accepted for publication in IEEE Sensors Journal. This is the author's version which has not been fully edited and
content may change prior to final publication. Citation information: DOI 10.1109/JSEN.2026.3724806

Photonic Sens, vol. 14, fasc. 2, p. 240202, giu. 2024, doi: 10.1007/s13320-024-0709-1.

[30] L. Guo, J. A. Jackman, H.-H. Yang, P. Chen, N.-J. Cho, e D.-H. Kim, «Strategies for enhancing the sensitivity of plasmonic nanosensors», *Nano Today*, vol. 10, fasc. 2, pp. 213–239, apr. 2015, doi: 10.1016/j.nantod.2015.02.007.

[31] I. B. Becerril-Castro *et al.*, «Gold Nanostars: Synthesis, Optical and SERS Analytical Properties», *Analysis & Sensing*, vol. 2, fasc. 3, p. e202200005, mag. 2022, doi: 10.1002/anse.202200005.

[32] L. Zu *et al.*, «Ultrasensitive and Multiple Biomarker Discrimination for Alzheimer's Disease via Plasmonic & Microfluidic Sensing Technologies», *Advanced Science*, vol. 11, fasc. 24, p. 2308783, giu. 2024, doi: 10.1002/advs.202308783.

[33] B. Kuswandi, Nuriman, J. Huskens, e W. Verboom, «Optical sensing systems for microfluidic devices: A review», *Analytica Chimica Acta*, vol. 601, fasc. 2, pp. 141–155, ott. 2007, doi: 10.1016/j.aca.2007.08.046.

[34] S. Zhang *et al.*, «In-situ growth of AuNPs on WS2@U-bent optical fiber for evanescent wave absorption sensor», *Applied Surface Science*, vol. 441, pp. 1072–1078, mag. 2018, doi: 10.1016/j.apsusc.2018.02.081.

[35] Z. Li *et al.*, «Evanescent wave absorption sensor with direct-growth MoS_2 film based on U-bent tapered multimode fiber», *J. Phys. D: Appl. Phys.*, vol. 50, fasc. 31, p. 315302, ago. 2017, doi: 10.1088/1361-6463/aa7b06.

[36] C. G. Khoury e T. Vo-Dinh, «Gold Nanostars For Surface-Enhanced Raman Scattering: Synthesis, Characterization and Optimization», *J. Phys. Chem. C*, vol. 112, fasc. 48, pp. 18849–18859, dic. 2008, doi: 10.1021/jp8054747.

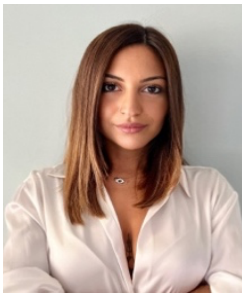
[37] M. Giardino, I. Mannelli, R. Yu, F. J. G. De Abajo, V. Pruneri, e D. Janner, «Synthesis of tailored nanostructured gold surfaces for SERS applications by controlled seed deposition and growth», *Applied Surface Science*, vol. 649, p. 159076, mar. 2024, doi: 10.1016/j.apsusc.2023.159076.

[38] P. Senthil Kumar, I. Pastoriza-Santos, B. Rodríguez-González, F. Javier García De Abajo, e L. M. Liz-Marzán, «High-yield synthesis and optical response of gold nanostars», *Nanotechnology*, vol. 19, fasc. 1, p. 015606, gen. 2008, doi: 10.1088/0957-4484/19/01/015606.

[39] F. Hao, C. L. Nehl, J. H. Hafner, e P. Nordlander, «Plasmon Resonances of a Gold Nanostar», *Nano Lett.*, vol. 7, fasc. 3, pp. 729–732, mar. 2007, doi: 10.1021/nl062969c.

[40] A. Vázquez Guardado, J. A. Ramirez Flores, G. Lopez-Galmiche, J. J. Escobedo Alatorre, e J. J. Sánchez-Mondragón, «Detection of Ethanol Concentration using a Generic Optical Sensor Platform», *CyS*, vol. 23, fasc. 1, p. 27, mar. 2019, doi: 10.13053/cys-23-1-3138.

[41] F. Chiavaioli, C. Gouveia, P. Jorge, e F. Baldini, «Towards a Uniform Metrological Assessment of Grating-Based Optical Fiber Sensors: From Refractometers to Biosensors», *Biosensors*, vol. 7, fasc. 2, p. 23, giu. 2017, doi: 10.3390/bios7020023.



Sharon Russo received the M.Sc. degree in Biomedical Engineering from Politecnico di Torino, Turin, Italy, in 2022. She is currently pursuing the Ph.D. degree in Materials Engineering at the Department of Applied Science and Technology (DISAT), Politecnico di Torino, which she joined in 2023. Her work focuses on the development of bioresorbable optical materials for theranostic applications. Her research interests include microfluidics, optical fiber-based biosensors, nanomaterials, and functional biomaterials for diagnostic and therapeutic biomedical technologies.



Nadia G. Boetti received the M.Sc. degree in Physics from the University of Turin, Italy, in 1998, and the Ph.D. degree in Electronic Devices from Politecnico di Torino, Italy, in 2014. She is a Technology Specialist in Optical Devices and Materials with Fondazione LINKS, Turin, Italy. Her research interests include specialty and bioresorbable optical fibers, rare-earth-doped glass materials for fiber lasers and amplifiers, and fiber Bragg grating (FBG) sensors for biomedical and structural health monitoring applications. She has led and participated in several national and international research projects in photonics, optical sensing, and biomedical technologies. She has authored or coauthored more than 150 scientific publications and has delivered invited talks at major international conferences organized by Optica and SPIE.



Matteo Giardino received his M.Sc. in Materials Engineering and his Ph.D. in Materials Science and Technology, with a focus on nanophotonics, from the Department of Applied Science and Technology (DISAT) at Politecnico di Torino.
Until January 2026, he worked as a Postdoctoral Researcher at the Alessandria Campus of Politecnico di Torino, where he developed novel Raman spectroscopy protocols for residual stress assessment in Al–Si alloys. In the frame of this activity, he has also been a Visiting Researcher at Kyushu University in Fukuoka, Japan, from August 2025 to December 2025, where he developed a correlative Raman–EBSD workflow to study residual stresses in AlSi10Mg thermally treated components.



Francesco Chiavaioli received the M.Sc. degree in telecommunications engineering and the Ph.D. degree in information engineering from University of Siena, Italy, in 2008 and 2012, respectively. From 2023, he is senior researcher at the National Research Council of Italy (CNR), Institute of Applied Physics "Nello Carrara". His research activities include optical sensors and biosensors, biophotonic platforms for molecule detection in life sciences, fiber optic probes, nanomaterials and nanostructures for sensing/biosensing and theranostic fiber probes. He has published more than 160 works in the mentioned fields. He has delivered more than 20 invited talks in National and International conferences and invited lectures. He is PI of several National and International projects on the topic of optical fiber sensing. He is Chair of SPIE Photonics Europe – Optical Sensing and Detection conference and is part of the Program Committee of OPTICA Bragg gratings, photosensitivity, and poling (BGPP) and Italian Conference on Optics and Photonics (ICOP). He is Editor of Optics and Laser Technology (Elsevier) and is Associate Editor of Measurement: Energy (Elsevier), Optics (MDPI) and Frontiers in Manufacturing Technology (Frontiers). He is part of the IEEE Sensors Council – Optical Sensors Cluster.



Davide Janner received the Ph.D. degree in physics from Politecnico di Milano in 2006 and the M.Sc. degree in physics from Università degli Studi di Milano, Milan, Italy, in 2002. During his Ph.D., he studied light propagation and its localization effects in periodic media both from a theoretical and experimental point of view. From 2006 till the end of 2015, he was at ICFO-The Institute of Photonic Sciences as a Junior Postdoctoral Researcher working on acoustooptic and electro-optic devices for telecommunication and sensing, specializing on techniques of micro- and nano-fabrication. Since 2015, he is an Associate Professor of materials science and his research topics are currently focused on bioresorbable and active glass materials for photonics applications, photonic sensors, and micro-/nano-structured multifunctional materials.

This work is licensed under a Creative Commons Attribution-NonCommercial-NoDerivatives 4.0 License.
For more information, see https://creativecommons.org/licenses/by-nc-nd/4.0/